Spectroscopic investigations of the nonequilibrium plasma and the charge flow in ion beam diodes

By Y. MARON, E. SARID, L. PERELMUTTER, M. E. FOORD, O. ZAHAVI, M. SARFATY, M. MARKOVITS, C. LITWIN AND E. NAHSHONI

Physics Department, Weizmann Institute of Science, 76100 Rehovot, Israel

(Received 10 July 1988)

Non-perturbing high resolution spectroscopic diagnostic methods have been developed to reliably measure the temporal and spatial distributions of physical quantities in the strong-field region and in the plasmas in pulsed-power devices. The methods were employed to investigate the properties of the acceleration gap and the behavior of the highly dynamic nonequilibrium anode plasma in intense ion diodes. Conclusions on the electron density and current density in the diode gap, the magnetic field induced by the current flow, the plasma conductivity, plasma heating, plasma expansion, particle fluxes and velocity distributions in the plasma, and possible use in other pulsed-power configurations are discussed.

1. Introduction

Understanding of the complicated phenomena that take place in a high power device can be improved only if high-resolution non-intrusive diagnostic methods are used to observe many physical quantities inside the device. In previous years we developed spectroscopic techniques capable of probing into both the acceleration gap (the region in which strong electric fields prevail) and the plasmas in pulsed-power systems (Maron et al. 1983; 1986; 1987; 1989a-d). These techniques were employed to investigate the charge flow and the anode-plasma behavior in magnetically insulated ion diodes.

This research programme was initiated by the suggestion (Maron et al. 1983) that the electric field distribution in the diode acceleration gap can be measured by the observation of the Stark shift of line emission from ions transversing the gap. Also, the Doppler line broadening parallel to the electrodes can give the transverse velocity distribution of the accelerated ions. For these measurements the ions can be excited by a tunable laser (Maron et al. 1983) or spontaneous line emission can be utilized. Using spontaneous emission, methods were developed to give the time dependent electric field distributions in planar ion diodes (Maron et al. 1986; 1987). This yielded the distributions of the ion density, of the electron density, and of the electron current density in the diode gap. Furthermore, the zero-field positions gave the time dependent actual width of the acceleration gap. This allowed comparisons with 1-D solutions (Antonsen & Ott 1976) to be made and also yielded the plasma expansion rate. The distributions of the electron density and the electron current density were observed to spread towards the anode beyond the region of the theoretical electron sheath. This explained the enhancement of the measured ion current density, over the calculated one. Furthermore, these measurements showed rapid gap closure early in the pulse resulting from expansion of the electric-field-excluding electrode plasmas. In addition, the transverse velocity distributions of C++ and Al++ ions in the diode acceleration gap

0263-0364/89/0704-0665\$05.00

were also obtained (Maron et al. 1987a). These velocities were found to be significantly smaller than previously observed for protons outside the diode.

Recently, we developed spectroscopic methods to investigate plasmas in a high power system (Maron et al. 1989a-d). For these investigations time dependent calculations of the particle excitations and ionizations proved to be essential. We obtained the ionic and neutral velocity distributions in the anode plasma from Doppler broadening and Doppler shift and the time dependent magnetic field from Zeeman splitting. The electron temperature and temperature gradient were determined from line intensities and collisional radiative calculations, that also accounted for the continuous injection of neutrals and multiply charged ions from the plasma source into the plasma. The time dependent absolute fluxes of the various species injected were also obtained. In this paper we focus on the measurements and the conclusions of the anode plasma, namely its formation, expansion, conductivity, heating, time-dependent composition, and the distributions of the particle densities and fluxes.

2. Experimental arrangement

We used a planar magnetically insulated diode (Maron et al. 1989a), shown in figure 1(a). The magnetic field B_2 was 5 to 9 kG and the diode waveforms are shown in figure 1(b). The anode plasma was formed as a result of a flashover of the epoxy-anode surface. Usually, light was collected from the anode plasma parallel to the magnetic field lines (see figure 1(c)). We used 1-meter spectrographs equipped with 2400 grooves/mm gratings, thus obtaining a spectral resolution ≤ 0.1 Å. Optical fibre-photomultiplier-tube arrays were used to obtain the spectral profiles of two lines in a single discharge with a temporal resolution of 5 ns.

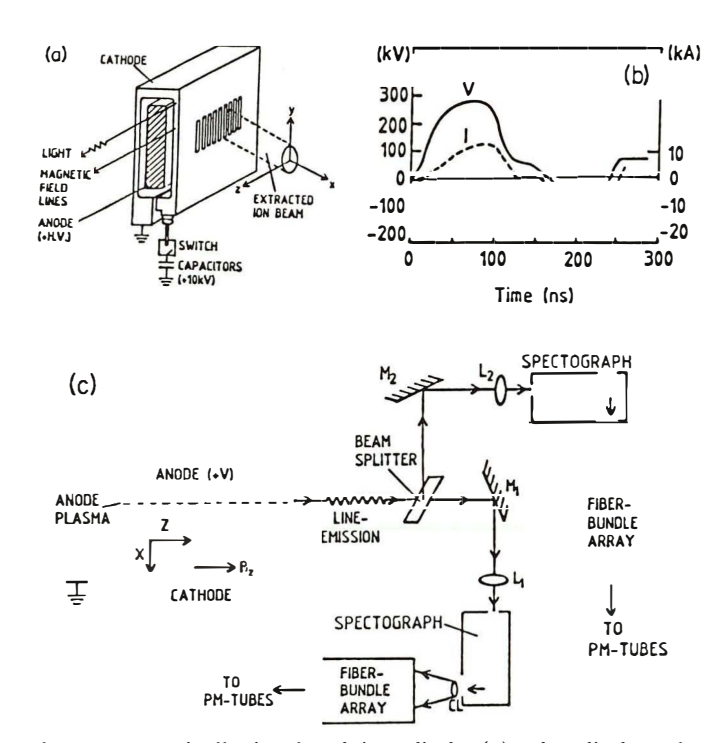


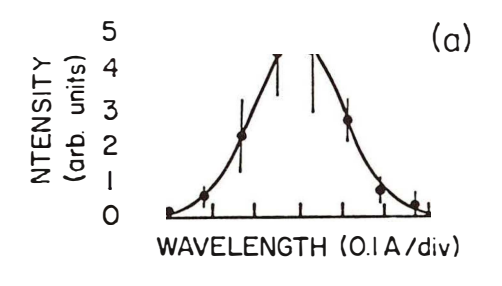
Figure 1. The planar magnetically insulated ion diode (a), the diode voltage and current waveforms for $B_z = 7.0 \text{ kG}$ (b), and the optical arrangement (c).

3. Plasma formation and early fast expansion

Line emission was first observed at t = 20 ns, and at t = 55 ns the plasma was seen to occupy about 1·5-mm-wide region near the anode surface, giving an expansion velocity ≥ 3 cm/ μ s, consistent with previous observations (Maron et al., 1986; 1987). Early fast plasma expansion against the magnetic field due to low-temperature (collisional) electrons is ruled out because of fast electron heating due to elastic collisions with the hotter ions (Litwin & Maron 1989). We therefore, suggested a mechanism of plasma expansion based on the formation of a fast-neutral layer by charge exchange processes and the subsequent ionization of this layer. The calculated expansion and ionization of this layer (Litwin & Maron 1989) were in agreement with the plasma thickness and density observed early in the pulse. This suggestion is consistent with the observed insensitivity of the plasma expansion to the applied magnetic field and the early presence of the magnetic field in the plasma (see Sec. 5).

4. Particle velocity distributions in the anode plasma

The particle velocity distributions in the anode plasma were determined by the observation of Doppler line broadening and shift (Maron et al. 1989a). The velocity distributions parallel to the anode were found to be nearly Maxwellian as shown in figure 2(a). The kinetic energies of neutrals and ions of various charge states were found to be about 8 eV and 20–80 eV, respectively. The ion temperature is significantly higher than what has been commonly believed. The Doppler line shift, parallel to and at an angle with the anode (see figure 2(b)) showed that the ions move away from the anode with nearly isotropic velocity distributions in half of the velocity space.



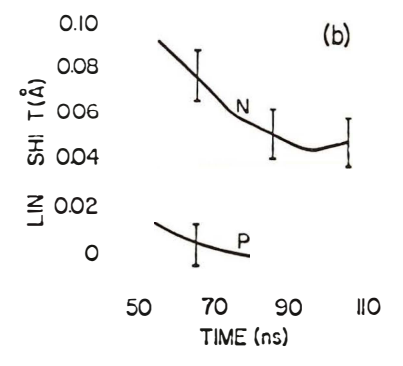


FIGURE 2. (a) Spectral profile of the CIII 2297 Å line for x = 1 mm and t = 85 ns and a best-fit Gaussian curve; (b) The blue shift of the CIII 2297 Å line measured at 53° with the normal to the anode (N) and the zero shift measured parallel to the anode (P).

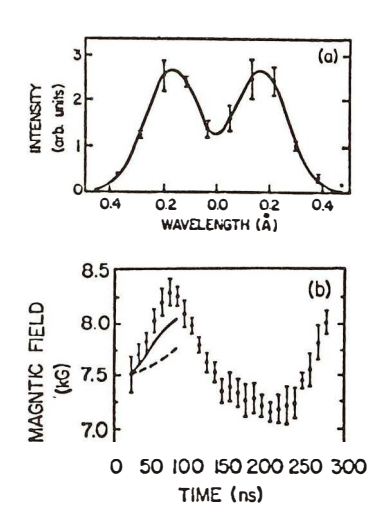


FIGURE 3. (a) Spectral profile of the BaII 6142 Å line observed with an applied magnetic field $B_z = 7.6 \,\mathrm{kG}$. The curve is a best fit of convolution of Gaussian profiles assumed for each of the emission components; (b) Magnetic field as a function of time within $0.1 \,\mathrm{mm}$ near the anode surface. Also given is the calculated magnetic-field rise at the anode surface for a classical plasma conductivity (dashed line) and an anomalous conductivity $10 \times \mathrm{lower}$ than the classical one (solid line).

Ion elastic collisions with the colder electrons cause substantial electron heating. The relatively large ion kinetic energies result in a high plasma pressure and thus a large plasma pressure-gradient. The latter enhances the plasma expansion against the magnetic field and also possibly affects the plasma stability (Maron *et al.*, 1989a), see Secs. 8 and 10.

5. The time dependent magnetic field in the plasma

The magnetic field in the anode plasma was measured by the observation of the Zeeman splitting of emission from BaII ions seeded in the plasma (see figure 3). The magnetic field applied in the diode was found to be present in the plasma a few nanoseconds after the plasma appeared. The rise of the magnetic field induced on the anode side by the electron flow in the diode gap was seen to be $\approx 0.8 \text{ kG}$ (see figure 3(b)), which is ≈ 3 times larger the prediction of the 1-D model (Antonsen & Ott 1976). However, it is consistent with the rise estimated (Maron *et al.* 1989b) using the pressure balance formula for the diode gap (Mendel & Quintez 1983), the measured ion current density, and the electric field distribution across the diode acceleration gap observed (Maron *et al.* 1986; 1987) for a similar diode configuration. Those observations showed significant electron flow close to the anode plasma, which should enhance the induced magnetic field on the anode side.

6. Electron temperature and temperature-gradient

Determination of the electron temperature in plasmas in short-pulse devices is difficult since such plasmas undergo rapid ionization. The latter, together with the continuous material flow into the plasma, that usually occurs in pulsed power devices (in our case material is injected from the dielectric surface, see Sec. 11), causes the excited-level populations and the level-population ratios to be time dependent and

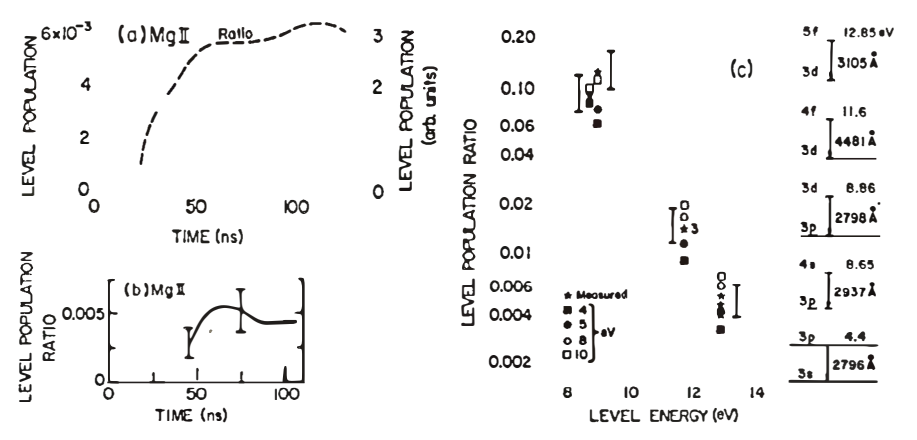


FIGURE 4. (a) The MgII $3p^2P_{3/2}$ population and the ratio of the $5f^2F$ population to the $3p^2P_{3/2}$ population, calculated using a continuous parabolic-in-time supply of MgII at the ground state. Populations are divided by the degeneracy. In these calculations $T_e = 7 \,\mathrm{eV}$ is assumed and the electron density used is the observed spatially averaged time dependent density; (b) The ratio of the MgII $5f^2F$ population (obtained from the 3105 Å line) to the $3p^2P_{3/2}$ population (2796 Å) measured in a single discharge; (c) Measured MgII level populations normalized to the population of the 3p level (that lies at $4\cdot4\,\mathrm{eV}$), averaged between t = 60 to 95 ns. The observed lines and the level energies in electronvolts are given in the level scheme. Also shown are the calculated normalized populations for $T_e = 4$, 5, 8, and $10\,\mathrm{eV}$ at $t \approx 80\,\mathrm{ns}$, using the continuous particle source for the plasma.

significantly different from the steady state values. Assuming a steady state for the level populations is shown (Maron *et al.* 1989c) to lead to misleading conclusions on the electron temperature and the charge state distributions.

We determined the electron temperature in our anode plasma by observing line intensities as a function of time and comparing them with time-dependent collisional-radiative calculations of the atomic level populations (Maron et al. 1989c; d). Important features of these calculations are that they use the electron density observed from the H_{β} Stark broadening and that they also account for the continuous material flow into the plasma. In these calculations atomic levels are coupled through electron collisional excitation and deexcitation and through spontaneous radiative decay. Each two adjacent atomic/ionic species are coupled through ionization and radiative/3-body recombinations. For carbon, dielectronic recombination into 2pnl excited states of CIII has also been included. Our modeling includes sufficient number of atomic levels. Higher-n levels up to the reduced continuum limit (Griem 1969) are assumed to be hydrogenic. The electron temperature was determined for times (the second half of the pulse) in which the line intensity ratios were seen to vary slowly both in the calculations (see figure 4(a)) and in the observations (see figure 4(b)), and were relatively insensitive to details of the continuous material flow into the plasma.

The electron temperature was determined independently from line intensities of three species: MgII, AlIII, and CIII. The results for all species yielded T_e between 5 to 8 eV, as shown in figure 5 for MgII. Furthermore, the dependence of the electron temperature on the distance x from the anode surface was obtained by observing the x-dependence of CIII line-intensity ratios. This is justified since the CIII propagation distance during the level-equilibration time (a few nanoseconds) is small with respect to the plasma thickness. These measurements showed that the electron temperature

670 Y. Maron et al.

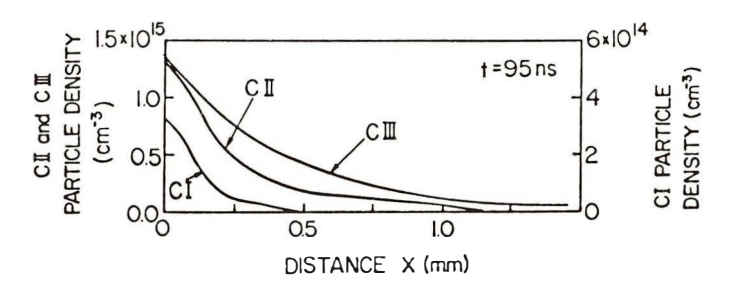


FIGURE 5. Calculated axial density distributions of CI, CII, and CIII for t = 95 ns obtained using the continuous particle supply into the plasma and assuming $T_e = 7$ eV.

varies by $<1\,\mathrm{eV}$ across the plasma. The implication of this result will be discussed in Sec. 9.

7. Anomalous plasma conductivity

Using the time dependent magnetic field rise on the anode side (see Sec. 5) we now calculate the penetration of the time dependent component of the magnetic field into the anode plasma. Assuming 1-D geometry and a constant plasma conductivity we calculate the rise of the magnetic field at the anode surface for a classical plasma conductivity, as shown in figure 3(b). The calculated rise of the magnetic field is significantly less than that observed. However, assuming an anomalous conductivity ($\approx 10 \times$ lower than classical, see Sec. 8) the calculated rise is much closer to the observed one, see figure 3(b). In Secs. 8 and 9 we present three additional observations in support of this conductivity.

8. Plasma expansion against the magnetic field

The measurement of the electric field distribution in the acceleration gap (Maron et al. 1986; 1987) indicated that after its early fast expansion (see Sec. 3) the anode plasma expanded at a rate $\approx 1 \text{ cm}/\mu\text{s}$. This rate agrees with the present observations (Maron et al. 1989a) and it is much higher than what had been expected from the plasma diffusion against the magnetic field.

Based on the present observations we now propose an explanation for this relatively fast plasma expansion. Since collisions with the neutral particles in the plasma are found to be insignificant and since the proton Larmor radius is smaller than the plasma thickness, we use the fluid equation for the expansion velocity of a fully ionized plasma

$$V_x = \frac{-c^2}{\sigma R^2} \, \partial_x P,$$

where P is the plasma pressure and σ is the plasma conductivity. Assuming $P = n(T_i + T_e)$ and using $T_i = 25 \, \mathrm{eV}$, $T_e = 7 \, \mathrm{eV}$, a plasma density $T_e = 2.2 \times 10^{15} \, \mathrm{cm}^{-3}$, a pressure-gradient scale of 1 mm, and $T_e = 7.2 \, \mathrm{kG}$ as observed in the plasma (Maron et al. 1989a-c), gives for a classical conductivity $T_e = 0.1 \, \mathrm{cm}/\mu$ s. This is much smaller than the observed velocity ($T_e = 10 \, \mathrm{cm}/\mu$ s). However, the use of an anomalous plasma conductivity that is $T_e = 10 \, \mathrm{cm}/\mu$ s conductivity explains the observed $T_e = 10 \, \mathrm{cm}/\mu$ s.

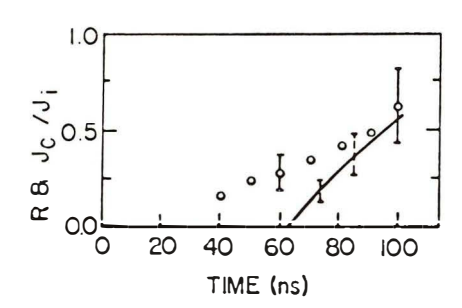


FIGURE 6. The calculated ratio R of the CIII charge flux to the total charge flux in the plasma for $x_0 = 1.5$ mm from the anode surface (curve) and the measured ratio J_c/J_i of CIII current to total current obtained from Faraday cup measurements outside the diode (circles).

particle injection into the plasma and the particle ionizations were found to be responsible for the observed rise in the plasma areal density (Maron et al. 1989d).

12. Particle fluxes from the plasma into the acceleration gap

Using the electron density (Maron et al. 1989a), electron temperature (Maron et al. 1989c), and particle fluxes (Maron et al. 1989d) determined, and the observed particle velocity distributions (Maron et al. 1989a), we calculated the ionization rates and the densities of ions and neutral particles as a function of time and position as they flow towards the outer region of the plasma (Maron et al. 1989d). These calculations predict that doubly charged ions and protons dominate the outer (ion-emitting) plasma region as shown in figure 5 for the carbon particles. This is consistent with Faraday cup measurements on the extracted ion beam.

Due to its relatively large concentration and high velocity, a significant fraction of the neutral hydrogen reaches the plasma outer region. A quantitative analysis shows that the ionization of hydrogen in the plasma front contributes a proton flux that is similar to the density of the proton current extracted into the diode acceleration gap. This proton flux due to hydrogen ionization may be important if the proton flow in the magnetized plasma, that is penetrated by the magnetic field (Maron *et al.* 1989c), is limited.

The ratio of CIII to proton fluxes is predicted to rise from a low value to about half towards the end of the pulse. This rise is found to agree with the observed time dependent CIII to proton ratio in the extracted ion beam as shown in figure 6.

13. Summary and conclusions

Spectroscopic diagnostic methods have been developed to measure physical quantities inside intense ion diodes. We determined the electric field distribution in the diode acceleration gap, the ion transverse velocity distributions in the gap, the velocity distributions of ions and neutral particles in the anode plasma, the average ion flow velocity in the plasma, the magnetic field penetration into the plasma, the magnetic field induced on the anode side by the electrons drifting in the diode acceleration gap, the electron temperature and temperature-gradient in the plasma, the time-dependent fluxes of various species of different charge states from the anode surface into the plasma, the time-dependent plasma composition, and the particle fluxes and densities in the ion-emitting plasma region.

From these observations we concluded that electrons in the diode acceleration gap

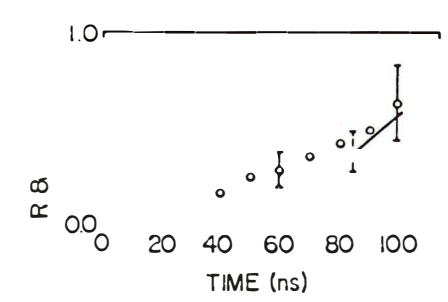


FIGURE 6. The calculated ratio R of the CIII charge flux to the total charge flux in the plasma for $x_0 = 1.5$ mm from the anode surface (curve) and the measured ratio J_c/J_i of CIII current to total current obtained from Faraday cup measurements outside the diode (circles).

particle injection into the plasma and the particle ionizations were found to be responsible for the observed rise in the plasma areal density (Maron et al. 1989d).

12. Particle fluxes from the plasma into the acceleration gap

Using the electron density (Maron et al. 1989a), electron temperature (Maron et al. 1989c), and particle fluxes (Maron et al. 1989d) determined, and the observed particle velocity distributions (Maron et al. 1989a), we calculated the ionization rates and the densities of ions and neutral particles as a function of time and position as they flow towards the outer region of the plasma (Maron et al. 1989d). These calculations predict that doubly charged ions and protons dominate the outer (ion-emitting) plasma region as shown in figure 5 for the carbon particles. This is consistent with Faraday cup measurements on the extracted ion beam.

Due to its relatively large concentration and high velocity, a significant fraction of the neutral hydrogen reaches the plasma outer region. A quantitative analysis shows that the ionization of hydrogen in the plasma front contributes a proton flux that is similar to the density of the proton current extracted into the diode acceleration gap. This proton flux due to hydrogen ionization may be important if the proton flow in the magnetized plasma, that is penetrated by the magnetic field (Maron *et al.* 1989c), is limited.

The ratio of CIII to proton fluxes is predicted to rise from a low value to about half towards the end of the pulse. This rise is found to agree with the observed time dependent CIII to proton ratio in the extracted ion beam as shown in figure 6.

13. Summary and conclusions

Spectroscopic diagnostic methods have been developed to measure physical quantities inside intense ion diodes. We determined the electric field distribution in the diode acceleration gap, the ion transverse velocity distributions in the gap, the velocity distributions of ions and neutral particles in the anode plasma, the average ion flow velocity in the plasma, the magnetic field penetration into the plasma, the magnetic field induced on the anode side by the electrons drifting in the diode acceleration gap, the electron temperature and temperature-gradient in the plasma, the time-dependent fluxes of various species of different charge states from the anode surface into the plasma, the time-dependent plasma composition, and the particle fluxes and densities in the ion-emitting plasma region.

From these observations we concluded that electrons in the diode acceleration gap

spread towards the anode beyond the theoretical electron sheath region and thus enhance the ion current densities and the magnetic field induced on the anode side. The ion transverse velocities in the diode gap are smaller than those outside the diode. Electron heating in the anode plasma is mainly due to the pressure-driven currents in the plasma and the electron elastic collisions with the hotter ions ($T_e \approx 7 \, \mathrm{eV}$ vs. $T_i \approx 20-80 \, \mathrm{eV}$). The observed fast plasma expansion against the magnetic field is explained by the observed plasma pressure gradient and an anomalous plasma conductivity $\approx 10 \times 10 \, \mathrm{eV}$ lower than the classical conductivity. This conductivity also explains the observed penetration of the time-dependent magnetic field into the plasma, the uniformity of the electron temperature in the plasma, and the balance between the electron heating and cooling rates (the electron cooling is dominated by inelastic collisions). The absolute fluxes of various species, determined as a function of time and position in the plasma, yielded predictions on the composition of the generated ion beam which were supported by Faraday cup measurements outside the diode.

Such studies can be used for the investigation of pulsed-power devices, for the design of plasma sources, and for studying plasma-wall interactions. The use of laser-induced-fluorescence with the geometry previously suggested (Maron *et al.* 1983) can be used to obtain better accuracy and to examine 2-D effects in the electric field distribution and in the plasma behavior.

REFERENCES

Antonsen, T. M. & Ott, E. 1976 Phys. Fluids 19, 52.

DAVIDSON, R. C. & GLADD, N. T. 1975 Phys. Fluids 18, 1327.

DAVIDSON, R. C. 1978 Phys. Fluids 21, 1375.

LITWIN, C. & MARON, Y. 1989 Phys. Fluids 81, 670.

MARON, Y. & LITWIN, C. 1983 J. Appl. Phys. 54, 2086.

MARON, Y. et al. 1986 Phys. Rev. Lett. 57, 699.

MARON, Y. et al. 1987 Phys. Rev. A36, 2818.

MARON, Y. et al. 1987a J. Appl. Phys. 61, 4781.

MARON, Y. et al. 1989a Phys. Rev. A.

Maron, Y. et al. 1989b Phys. Rev. A.

MARON, Y. et al. 1989c Phys. Rev. A.

MARON, Y. et al. 1989d Phys. Rev. A.

MENDEL, C. W. & QUINTEZ, J. P. 1983 Comments on Plasma Phys. Controlled Fusion 8, 43.